Available online at www.sciencedirect.com
SCIENCE DIRECT
Journal of Molecular Catalysis B: Enzymatic 39 (2006) 171–178
JOURNAL OF MOLECULAR CATALYSIS B: ENZYMATIC
www.elsevier.com/locate/molcatb

Exploring the cupin-type metal-coordinating signature of acetylacetone dioxygenase Dke1 with site-directed mutagenesis: Catalytic reaction profile and Fe^{2+} binding stability of Glu-69 → Gln mutant

Grit D. Straganz [a,*], Sigrid Egger [a], Gianluca Aquino [c], Sabato D'Auria [c], Bernd Nidetzky [a,b,**]

[a] *Institute of Biotechnology and Biochemical Engineering, Graz University of Technology, Petersgasse 12, A-8010 Graz, Austria*
[b] *Research Centre Applied Biocatalysis, Graz University of Technology, Petersgasse 12, A-8010 Graz, Austria*
[c] *Institute of Protein Biochemistry, National Research Council C.N.R., Via Pietro Castellino 111, 80131 Naples, Italy*

Available online 28 February 2006

Abstract

Glu-69 belongs to a proposed active-site consensus motif His^{62}-X-His^{64}-X_4-Glu^{69} (where X is any amino acid) that acetylacetone dioxygenase Dke1 from *Acinetobacter johnsonii* shares with structurally related non-heme metal enzymes of the cupin protein superfamily. We report functional consequences of the site-directed replacement Glu-69 → Gln based on a detailed biochemical and kinetic characterization of the purified Dke1 mutant. Perturbations of the free energy profile of the wild-type caused by the mutation were surprisingly small, with key points of the reaction pathway such as β-diketone substrate binding, the rate-limiting reduction of dioxygen, and C–C bond cleavage essentially left unaltered. Release of Fe^{2+} from the mutant active site occurred at twice the wild-type rate, and the thermal stability of β-sheet secondary structure in Fe^{2+}-depleted apo-proteins was lower in the mutant. The substitution Glu-69 → Gln is thus remarkably silent regarding Dke1 function. These results do not support a unified catalytic or metal-coordinating role of Glu-69 (and its positional homologues) in O_2-dependent cupin-fold enzymes.

Keywords: Non-heme iron; C–C-bond cleavage; β-Diketone; Cupin; Metalloenzyme

1. Introduction

The enzymatic activation of dioxygen is crucial for all aerobic life in nature. Mononuclear non-heme metal active sites master the intricate chemistry of dioxygen to bring about a wide range of substrate transformations, which include the cleavage of C–C single and double bonds; hydroxylation; decarboxylation; and C–C bond formation [1]. High-resolution structural studies have revealed a common theme of non-heme metal coordination in enzymes that are unrelated by sequence and differ in three-dimensional fold. Two types of non-heme metal sites are found, apparently as a result of convergent evolution. The type 1 site is composed of two histidine and one carboxylate ligands [2]. The type 2 site contains three coordinating histidine residues whereby an additional carboxylate has a strongly conserved position close to the metal but not strictly coordinating it [3–5] (Fig. 1a).

The known, structurally characterized type 2 non-heme metal enzymes have a β-barrel (or "jelly roll") fold and belong to the cupin protein superfamily. Two consensus motifs have been proposed, which provide the signature for cupin metalloproteins (Fig. 1b): G-X-**H**-X-**H**-$X_{3,4}$-**E**-X_6-G and G-$(X)_5$-P-X-G-$(X)_2$-**H**-$(X)_3$-N where X is any amino acid and the key residues in the metal's first coordination shell are highlighted in bold. Dijkstra and co-workers have determined structure–function relationships for the side chains of the cupin signature based on their thorough studies of a fungal Cu^{2+}-dependent quercetin dioxygenase. The histidine residues are coordinating the metal cofactor, and the glutamate was assigned multiple probable functions: acid–base catalysis; proton relay; and modulator of the redox potential of the metal [14].

The β-diketone-cleaving enzyme Dke1 (EC 1.13.11.50) is a non-heme Fe^{2+}-dependent dioxygenase from *Acinetobacter johnsonii* [12,13]. It catalyzes the O_2-dependent conversion of

* Corresponding author. Tel.: +43 316 873 8414; fax: +43 316 873 8434.
** Corresponding author. Tel.: +43 316 873 8400; fax: +43 316 873 8434.
E-mail addresses: grit.straganz@tugraz.at (G.D. Straganz), bernd.nidetzky@tugraz.at (B. Nidetzky).

1381-1177/$ – see front matter © 2006 Elsevier B.V. All rights reserved.
doi:10.1016/j.molcatb.2006.01.019

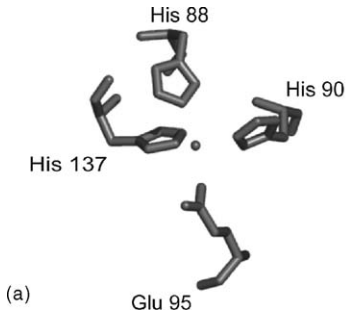

(b)

GER	--TNPP**H**I**H**PRAT**E**IGMVMKG GETFVIPRGLM**H**FQFN
ODC	GAIREL**H**W**H**KNA-**E**WAYVLKG GDLWYFPPGIP**H**SLQA
GDO	GEVAPT**H**R**H**SQSALRFVVD-G GDFVITPPWAW**H**DHVN
CDO	NKETTV**H**D**H**GQSIGCAMVLEG GECLISTKGLI**H**KMSN
ARD	EKFLNE**H**T**H**GE-D**E**VRFFVEG NDLISVPAHTP**H**WFDM
QDN	ALGVLP**H**I**H**QKHY**E**NFYCNKG GDYGSVPRNVT**H**TFQI
DKE	GSSFAS**H**I**H**AGPG**E**Y-FLTKG PSYGFESSGAL**H**GKTF
Consensus	G **H H** **E** G GD P G **H** N

Fig. 1. Typical active-site organisation and two consensus motifs for O_2-dependent metalloenzymes of the cupin protein superfamily. Panel (a): type 2 metal coordination by three histidine residues with a glutamate residue juxtaposed, exemplified by the active site of germin (Mn^{2+}-dependent oxalate oxidase) [6] and Panel (b): a multiple sequence alignment to underpin the conserved motifs in O_2-dependent cupin metalloenzymes. GER, oxalate oxidase [6]; ODC, oxalate decarboxylase [7]; GDO, gentisate dioxygenase [8]; CDO, cysteine dioxygenase [9]; ARD, acireductone dioxygenase [10]; QDN, quercetin dioxygenase [11]; DKE, diketone cleaving enzyme Dke1 [12,13], whereby for GDO and CDO no structural data are available. Note that the glutamate homologous to Glu-69 of Dke1 is conserved in all reported structures of type 2 oxygenases, while sequence alignments suggest an 'only' ∼70% conservation.

acetylacetone (2,4-pentanedione; PD) into methylglyoxal and acetate (Scheme 1).

Dke1 has a broad substrate specificity. It can accept β-diketones that represent a wide variety of substituents at both the central C-3 and the methyl groups of the natural PD substrate. Oxidative C–C bond cleavage in β-diketones proceeds with stoichiometric consumption of O_2, and one atom from dioxygen is incorporated into each reaction product upon the enzymatic bond fission. The primary structure of Dke1 clearly contains the cupin signature, with limited diversity noted in the second consensus motif (Fig. 1b). His-62, His-64 and His-104 are thus the putative ligands to Fe^{2+}. The X-ray crystal structure of an inactive form of Dke1 in which Fe^{2+} was replaced by adventitious Zn^{2+} supports a role of the three histidine residues in metal coordination [17]. The residue Glu-69, unlike its positional homologues in other cupin metalloenzymes, wholly points away from the metal cofactor in the Zn^{2+} structure, raising the question of what its function in native Dke1 could be.

The proposed catalytic pathway of oxidative C–C bond cleavage is summarized in Scheme 1. The β-diketone substrate binds to the active site where it forms a metal-to-ligand charge transfer (MLCT) complex with Fe^{2+}. β-Dicarbonyls that are of physiological relevance generally have a pK_a of ∼9 and are likely to enter the active site in a charge neutral form [16]. Loss of a proton upon coordination as a monoanionic *cis*-β-keto-enolate to Fe^{2+} may require the participation of protein side chains, arguably that of Glu-69. The chemical transformation of the Fe^{2+}-bound substrate into an alkyl peroxidate intermediate is the rate-limiting step of the reaction catalyzed by the wild-type [16]. In this critical conversion, the catalytic reduction of dioxygen is performed. Finally, the peroxidate carries out intramolecular nucleophilic attack on the juxtaposed carbonyl groups, preferring the most electron-deficient of the two, to generate a dioxetane which then decomposes into the products. Glu-69 could take part in oxygen chemistry or the ensuing bond cleavage.

In this paper, site-directed mutagenesis was used to replace the original side chain of Glu-69 with the side chain of Gln, and the functional consequences in a purified Dke1 point mutant were analyzed in detail at different points of the reaction coordinate, as outlined in Scheme 1 and using methods previously established with the wild-type enzyme [15,16]. The results for Dke1 reveal that the positionally conserved Glu-69 is not always essential for enzyme function in cupin-fold type 2 metalloenzymes.

2. Material and methods

2.1. Materials

2,4-Pentanedione (PD), 1,1,1-trifluoro-PD (TFPD), 4,4-difluoro-1-phenyl-1,3-butanedione (DFPB), 4,4,4-trifluoro-1-phenyl-1,3-butanedione (TFPB), phenyl-1,3-butanedione (PB) and other chemicals were from Sigma Aldrich (St. Louis, MO, U.S.A.) except 1,1-difluoro-2,4-pentanedione (DFPD) which was from Matrix Scientific (Columbia, SC, U.S.A.). All chemicals were of the highest available quality and unless otherwise mentioned greater than 97% pure. *Pfu* DNA polymerase was from Promega (Madison WI, U.S.A.). *Dpn*I was obtained from MBI Fermentas (St. Leon-Rot, Germany). The other enzymes for molecular biology and the expression vector pKYB1 were from New England Biolabs (Beverly, MA, U.S.A.).

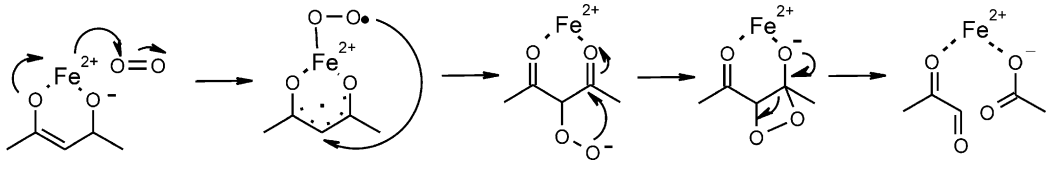

Scheme 1. Proposed reaction mechanism for Dke 1. The scheme is based on results of prior studies of the wild-type enzyme [13,15,16].

2.2. Methods

2.2.1. Site-directed mutagenesis and enzyme preparation

A reported two stage PCR protocol was used to introduce the site-directed mutation [18]. The plasmid vector pKYB1-*dke1_Strep* [19] was used as a template. It contains the full-length *dke1* gene fused to an oligonucleotide encoding a 10-amino acid C-terminal affinity tag [20]. Note that the biochemical properties of Dke1 are not influenced by the tag [19]. For PCR, two separate primer extension reactions were performed using the forward (5′-CATGCTGGCCCCGGGCAATATT-TCCTGACTAAGGGAAAAATG-3′) and reverse (5′-GT-CAGGAAATATTGCCCGGGG-CCAGCATGAATATGAG-3′) oligonucleotide primer, respectively, whereby the mismatched bases in each primer are underlined. The PCR protocol used 270 ng of template in a total volume of 50 μL. Four cycles of separate amplification with 3 U of *Pfu* DNA polymerase (Promega, Madison WI, U.S.A.) were followed by 18 cycles of amplification of the combined reaction mixtures using an annealing temperature of 62 °C. The final extension phase was 15 min at 72 °C. After digestion of the template DNA with *Dpn*I, the amplified plasmid vectors were transformed into electro-competent cells of *E. coli* BL21(DE3) according to protocols provided by the manufacturer (Stratagene, La Jolla, CA, U.S.A.). Plasmid miniprep DNA from positive clones was subjected to dideoxy sequencing of the entire *dke1* gene to verify that the desired mutation had been introduced and no base misincorporations had occurred because of DNA polymerase errors.

Production of recombinant wild-type Dke1 and the mutant Glu-69 → Gln used the procedures described recently [19]. Purification was carried out according to reported protocols using affinity chromatography with a 1-mL *Strep*-Tactin column (IBA, Goettingen, Germany). Stock solutions of wild-type and mutant enzymes were stored in 20 mM Tris/HCl buffer, pH 7.5, at protein concentration of approximately 10 mg mL^{-1}. Highly concentrated protein solutions (≥10 mg mL^{-1}) were prepared with Vivaspin centrifugation concentrator tubes (Vivascience, Hannover, Germany).

2.2.2. Enzyme assays and steady-state kinetic studies

Unless mentioned otherwise, a 20 mM Tris/HCl buffer, pH 7.5, was used. The standard assay of Dke1 activity was carried out at 25 °C and used 0.2 mM PD dissolved in air-saturated buffer as the substrate and measured spectrophotometrically at 280 nm the rate of substrate conversion at 25 °C. Steady-state kinetic studies with PD and TFPD were performed by recording the initial rate of substrate consumption with a DU 800 UV–vis Spectrophotometer (Beckmann Coulter, Inc., Fullerton, CA, U.S.A.) at the wavelength of maximum absorbance of the respective β-diketone: PD (280 nm); TFPD (290 nm). Kinetic parameters were obtained from either a series of initial-rate measurements at varied substrate concentrations and a non-linear fit of the Henri–Michaelis–Menten equation for a single-substrate enzymatic reaction to the data, or by applying the integrated form of this equation to expanded reaction time courses. Note that dioxygen was always present in about five-fold excess (260 μM). It was proven that both approaches of kinetic analysis yielded consistent estimates for the catalytic centre activity (k_{cat}) and the Michaelis–Menten constant (K_m).

2.2.3. Substrate binding and single turnover kinetics

2.2.3.1. Absorbance. An anaerobic solution of Glu-69 → Gln mutant (100 μM Fe^{2+}-containing active sites) in 20 mM Tris/HCl buffer, pH 7.5, was prepared in an evacuable quartz cuvette sealed with a septum. Spectroscopic titrations were carried out by adding aliquots of 0.5–5 μL from an anaerobic stock solution of ligand with a Hamilton syringe. Absorbance wavelength scans in the range 300–700 nm were carried out on the free enzyme and after each addition of ligand, and the resulting spectra were compared after appropriate corrections for dilution. The Beckman spectrophotometer was used. Controls were obtained by the same procedure without enzyme, and blank values at the corresponding ligand concentrations were subtracted in all cases.

2.2.3.2. Fluorescence. Measurements at 4 °C were carried out with a Hitachi F-4500 Fluorescence Spectrophotometer (Hitachi High-Technologies, Tokyo, Japan) using excitation and emission wavelengths of 290 and 330 nm, respectively. Constant slit widths of 5 nm were used. The quenching of the intrinsic protein tryptophan fluorescence was measured in dependence of the ligand concentration (c_L). The concentration of Fe^{2+}-containing active sites of the Glu-69 → Gln mutant was 0.2 μM. After corrections for dilution and blank readings, data were plotted as $(I_0-I)/I_0$ against c_L, where I_0 and I are fluorescence intensities in the absence and in the presence of ligand, respectively.

2.2.3.3. Dissociation constants. Equilibrium binding experiments performed in the presence of a high enzyme concentration ($c_e > 100$ μM) lead to conditions in which a significant portion of the total concentration of each binding partner is tied in the binary complex. The approximation that $c_e \ll c_L$ is no longer valid, and thus c_L at binding equilibrium is different from the total ligand concentration. Eq. (1) was therefore used to determine the dissociation constant (K_d):

$$A_\lambda = \frac{\varepsilon((K_d + c_e + c_L) - ((K_d + c_e + c_L)^2 - 4c_e \cdot c_L)^{0.5})}{2} \quad (1)$$

where A_λ is the absorbance of the binary enzyme–ligand complex at a characteristic wavelength (see Section 3) with a corresponding molar absorption coefficient ε, c_e is the total concentration of enzyme active sites and c_L is the total ligand concentration.

2.2.3.4. Single turnover kinetics. The O_2-dependent breakdown of the enzyme–substrate complex was measured spectrophotometrically, at 455 nm (see Section 3), under conditions in which the available substrate concentration ($c_{TFPD} = 90$ μM) was limiting the reaction to less than a single turnover of the enzyme (100 μM Fe^{2+}-containing active sites of Glu-69 → Gln mutant). Note, however, that the substrate concentration was

fully saturating at the steady-state ($K_m \approx 5\ \mu M$). The reaction was carried out at 25 °C in an air-saturated 20 mM Tris/HCl buffer, pH 7.5, and the time course of decay of the colored complex was monitored.

2.2.4. Fe^{2+} content and Fe^{2+} release kinetics

The content of protein-bound Fe^{2+} in purified preparations of wild-type Dke1 and Glu-69 → Gln mutant was determined by employing a colorimetric assay that used formation of a colored solution complex between Fe^{2+} and ferene S for detection and was described elsewhere in detail [21,22]. The molar absorption coefficient for the complex at 592 nm was 35.5 $mM^{-1}\ cm^{-1}$. All measurements were performed in 20 mM Tris/HCl buffer, pH 7.5, containing 20 mM L-ascorbic acid to maintain a completely reduced state for the released iron over time. The experiment was designed as an end-point determination whereby absorbance at 592 nm (A_{592}) was recorded after exhaustive incubation times of 2–5 h or as a time course measurement in which the increase in A_{592} was monitored on-line in the spectrophotometer.

2.2.5. Circular dichroism spectroscopic studies

Wild-type and mutant enzymes were incubated at 30 °C until the specific activity had dropped to less than 5% of the original value. Proteins were gel-filtered and shown to lack detectable amounts of bound Fe^{2+}. Solutions of the apo-forms of wild-type Dke1 and Glu-69 → Gln mutant were prepared in Tris/HCl buffer, 20 mM, pH 7.5, containing about 0.2 mg mL^{-1} protein. CD spectroscopy was performed with a Jasco J-710 spectropolarimeter that was equipped with a Neslab RTE-110 temperature-controlled liquid system. It was calibrated with a standard solution of (+)-10-camphosulfonic acid. Sealed cuvettes with 0.1 cm pathlength were used. Photomultiplier high voltage did not exceed 600 V in the spectral regions measured. Each spectrum was averaged five times and smoothed with Spectropolarimeter System Software. All measurements were performed under nitrogen flow. Before undergoing CD analysis, the respective sample was kept at the temperature being studied for 6 min. The results are expressed in terms of residue molar ellipticity.

3. Results and discussion

3.1. Purification and characterization of Glu-69 → Gln mutant

Recombinant wild-type Dke1 and the Glu-69 → Gln mutant thereof were produced under identical culture conditions, as described in Section 2. In each case, analysis by SDS-PAGE of the induced *E. coli* cell extract showed a strong protein band migrating to the expected position of approximately 18 kDa for the full length enzyme with the additional C-terminal Strep-tag (results not shown). Wild-type and mutant were purified efficiently using a single step of affinity chromatography in yields of approximately 80%. Fig. 2 shows the apparent electrophoretic homogeneity of the isolated enzymes. Unlike the wild-type which contained ≈1 Fe^{2+} per each protein subunit,

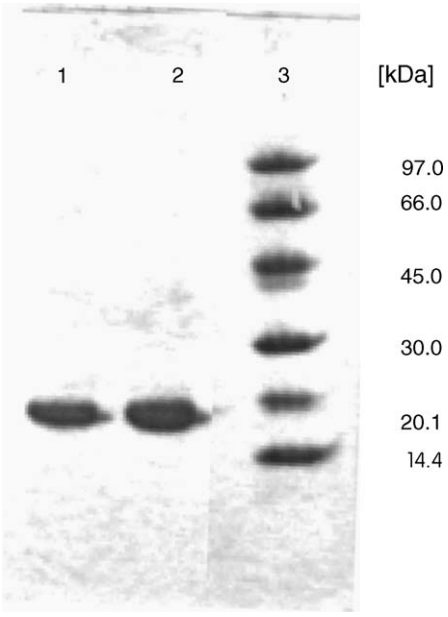

Fig. 2. Enzyme purification documented by SDS-PAGE. Purified preparations of Dke1 (~2 μg protein) were subjected to SDS-PAGE electrophoresis and subsequently visualized by Coomassie blue stain. Lane 1, wild-type Dke1; lane 2, Glu-69 → Gln mutant; lane 3, molecular mass standards.

metal cofactor binding in purified Glu-69 → Gln was consistently sub-stoichiometric (40–60%).

CD spectra of apo-forms of wild-type Dke1 and the mutant thereof were recorded at identical protein concentrations (0.25 mg mL^{-1}) and are superimposed in Fig. 3. The spectrum of the wild-type with a minimum at 210 nm and maximum at 230 nm is consistent with the predominant β-sheet secondary structural composition of the enzyme, known from the X-ray structure [17]. The spectrum of the mutant is similar to the wild-type spectrum, suggesting that the site-directed replacement did not cause substantial unfolding or other significant

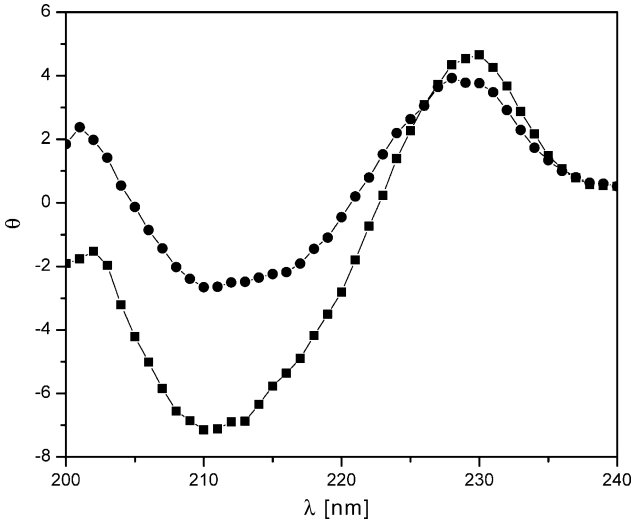

Fig. 3. Comparison of CD spectra of wild-type Dke1 and Glu-69 → Gln mutant. The spectra were recorded at 20 °C using a constant protein concentration of 0.25 mg mL^{-1} dissolved in 20 mM Tris/HCl buffer, pH 7.5. Results are expressed in terms of residue molar ellipticity (Θ).

Table 1
Comparative characterization of wild-type Dke1 and the Glu-69 → Gln mutant

Enzyme	k_{cat} (s^{-1})	K_m (μM)	k_{rel} (min^{-1})
Wild-type	6.6	6.0	0.1
Glu-69 → Gln	3.6	6.5	0.2

Kinetic parameters for the conversion of PD at 25 °C are reported. k_{rel} is the pseudo first-order rate constant of Fe^{2+} release from the active site.

changes in the content of elements of secondary structure. Interestingly, however, the intensities of the strongest CD bands at 210 and 230 nm were, respectively, increased and decreased in the spectrum of Glu-69 → Gln, compared with the wild-type spectrum, perhaps reflecting a less compactly folded structure of the mutant.

Initial rates of PD cleavage by wild-type and mutant were recorded under conditions in which the substrate concentration was varied and the concentration of O_2 was constant at 260 μM, reflecting air saturation at atmospheric pressure. Saturation in dioxygen was not attempted because the steady-state conversion rate of the wild-type is linearly dependent on the O_2 concentration [16]. Kinetic parameters were obtained by fitting the Michaelis–Menten equation to the data. They are summarized in Table 1 using appropriate correction for the molarity of Fe^{2+}-containing active sites present in the steady-state kinetic assays. The catalytic center activity (k_{cat}) of Glu-69 → Gln was half that of the wild-type value whereas apparent substrate binding (K_m) was hardly affected by the mutation.

3.2. Substrate binding and metal-to-ligand charge transfer

Prior studies of wild-type Dke1 have shown that quenching of intrinsic protein fluorescence is a suitable reporter of β-dicarbonyl substrate binding to the active site [16]. Results of anaerobic fluorescence titrations of wild-type and Glu-69 → Gln with TFPD, as shown in Fig. 4, were fitted with a rectangular hyperbola. The thus obtained apparent dissociation constants (K_d) were 6.7 [16] and 5.5 μM, respectively, suggesting that the mutation had no significant disruptive effect on substrate binding steps in the Dke1 catalytic cycle. Comparison of K_d values of wild-type and Glu-69 → Gln for another slow substrate TFBP confirm this notion and were 2.2 and 2.3 μM, respectively.

Under fully anaerobic conditions in which the dioxygenase reaction cannot take place or when using a very slow substrate that does not undergo O_2-dependent enzymatic conversion within the time domain of a titration experiment (≤5 min), incubation of wild-type Dke1 with a β-dicarbonyl ligand was accompanied by the appearance of two to three new absorbance bands that were not seen in the free enzyme [16].

Coordination of the β-diketone, as a *cis*-β-keto-enolate, to protein-bound Fe^{2+} and the resulting metal-to-ligand charge transfer were proposed to cause the change in the absorbance spectrum of the binary complex, compared with the spectrum of the unliganded wild-type enzyme. Fig. 5 (Panel a) shows differ-

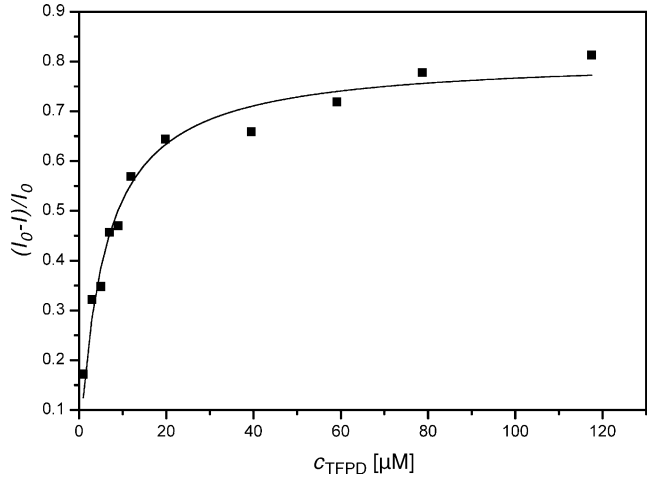

Fig. 4. Dissociation constant of the complex of Glu-69 → Gln and TFPD determined by anaerobic fluorescence titrations. Fluorescence emission was recorded at 330 nm, following excitation at 280 nm. Experiments were performed in 20 mM Tris/HCl buffer, pH 7.5, at 4 °C. The enzyme concentration was 0.2 μM.

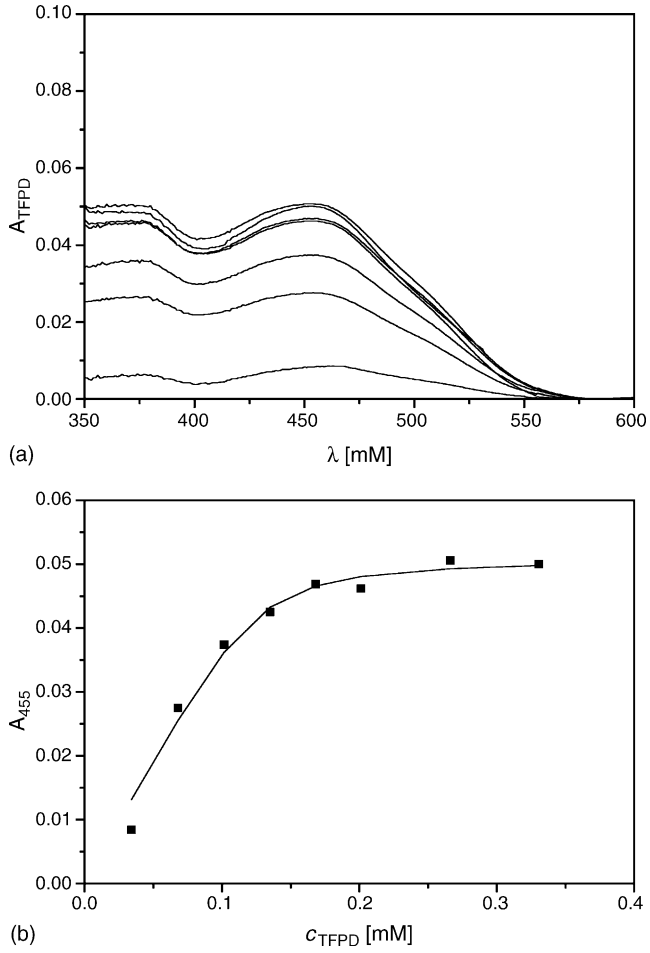

Fig. 5. Anaerobic spectrophotometric titration of Glu-69 → Gln mutant with TFPD and determination of the dissociation constant of the enzyme–TFPD complex. Panel (a): wavelength scans performed with Glu-69 → Gln at 25 °C before and after addition of TFPD. An anaerobic enzyme solution (125 μM) in 20 mM Tris/HCl buffer, pH 7.5, was used. Incremental amounts of TFPD were added up to a final concentration of 0.33 mM. Substrate binding leads to two new bands at 376 and 455 nm and Panel (b): plot of the increase in band intensity at 455 nm as a function of the total TFPD concentration. The full line shows a fit of Eq. (1) to the data. The shown TFPD concentrations correspond to the spectra in Panel (a).

ence spectra of Glu-69 → Gln mutant titrated with incremental amounts of TFPD until a two-fold molar excess of ligand was present. The spectrum of free Glu-69 → Gln was used as a reference.

The results reveal MLCT band appearance at approximately 376 and 455 nm in the spectrum of Glu-69 → Gln mutant, obviously in immediate response to addition, hence binding of ligand. The position of the lowest-energy MLCT band in the spectrum ($\lambda_{max} = 445 \pm 3$ nm) and its estimated molar extinction coefficient ($\varepsilon \approx 0.3\,mM^{-1}\,cm^{-1}$) were quite similar for wild-type and mutant, suggesting that electronic enzyme–substrate interactions at the binary complex level were not strongly altered by the site-directed replacement. Fig. 5 (Panel b) shows results of absorbance titration experiments in which the increase in MLCT band intensity was used to monitor substrate binding. Non-linear fits of Eq. (1) to the data yielded a K_d value of 5.1 μM for Glu-69 → Gln, in excellent agreement with the value determined via fluorescence titration.

3.3. O_2-dependent conversion of the enzyme–substrate complex

Fig. 6 shows time courses of the conversion of enzyme-bound TFPD, measured as decay in the MLCT band at 455 nm, under conditions in which the dioxygenase reaction was restricted by substrate limitation to a single turnover of the enzyme present.

At a dioxygen concentration of 260 μM, the co-substrate did not limit the progress of the reaction. A single exponential of the form $A_{455(t)} = A_{455(0)}\ \exp(-k_{obs} \cdot t)$ where k_{obs} is a pseudo first-order rate constant could describe the experimental absorbance traces very well, and non-linear fits to the data yielded a k_{obs} value of $8 \times 10^{-4}\,s^{-1}$. The corresponding k_{cat} value for the conversion of TFPD under steady-state conditions (when substrate was present in large molar excess over enzyme) was $1 \times 10^{-3}\,s^{-1}$. Therefore, these results imply that the O_2-dependent transformation of the enzyme-bound substrate, suitably positioned through coordination with the Fe^{2+} cofactor, is the rate-limiting step of the overall catalytic cycle of TFPD conversion by Glu-69 → Gln mutant. As indicated in Scheme 1, the formation of the peroxidate intermediate involves catalytic chemistry of dioxygen reduction. Wild-type Dke1 shows a k_{cat} for the reaction with TFPD of $4.3 \times 10^{-3}\,s^{-1}$ and the value of k_{obs} is $5.3 \times 10^{-3}\,s^{-1}$ [16]. In conclusion, therefore, substitution of Glu-69 has not changed the location of the rate-determining step in the catalytic pathway of the mutant, compared with that of the wild-type.

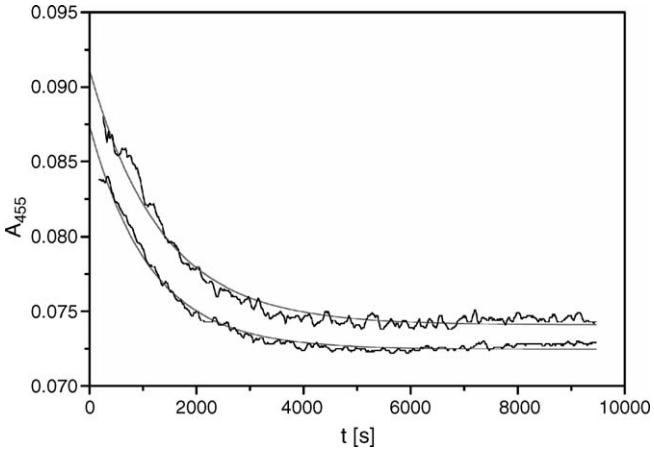

Fig. 6. Time courses of O_2-dependent conversion of enzyme-bound TFPD in single turnover kinetic experiments for Glu-69 → Gln mutant. The absorbance traces show the decay of the MLCT band at 455 nm which is a measure of binary complex formation (see Fig. 5, Panel (b)) and is thought to be characteristic of interactions between the metal cofactor and the *cis*-β-keto-enolate form of the substrate. Reactions were performed at 25 °C in 20 mM Tris/HCl buffer, pH 7.5, using 100 μM Fe^{2+}-containing enzyme active sites and 90 μM TFPD. The grey lines show the fit of a single exponential to the experimental data. The constant value obtained after exhaustive conversion of substrate reflects the basal absorbance of the buffered enzyme solution.

3.4. Bond cleavage selectivity

Recent studies have revealed a strong electronic substituent effect on the C–C bond cleavage specificity of wild-type Dke1 [15]. An analogous analysis of the cleavage pattern for the degradation of asymmetric β-dicarbonyl substrates showed a marked preference for enzymatic fission of the bond adjacent to the most electron-deficient carbon. In the case of the Dke1-catalyzed conversion of TFPD, for example, trifluoro-acetate and methylglyoxal are the predominant products and only small amounts of acetate and trifluoro-methylglyoxal are formed. The enzymatic selectivity for cleavage at the two candidate C–C bonds in substituted β-diketones could be correlated with the difference in the Taft factors of the substituents ($\Delta\sigma^*$). The resulting linear free energy relationship is mechanistically diagnostic and led to the proposal of a reaction pathway via a dioxetane. A possible role of Glu-69 in C–C bond cleavage was considered. Nucleophilic attack on a carbonyl carbon requires a deprotonated peroxidate whose pK_a can be estimated from literature values to be in the range 10–11. Because the enzymatic reaction proceeds optimally at pH ≈ 7 the active site of Dke1 obviously prevents protonation of the peroxidate from the bulk solvent. The position of the side chain of Glu-69 could thus be a determinant of the intermediacy of a dioxetane. Fig. 7 shows a correlation of the logarithmic cleavage ratios and $\Delta\sigma^*$. A straight-line fit to the data gave a slope value of 0.68 with a good correlation coefficient of 0.98. By way of comparison, a similar correlation for the wild-type had a slope of 0.54. The replacement Glu-69 → Gln did not change C–C bond cleavage specificity of Dke1.

3.5. Fe^{2+} release kinetics

Fig. 8 compares time courses of Fe^{2+} dissociation from active sites of wild-type and Glu-69 → Gln at room temperature in the presence of a 1000-fold molar excess of the chelating ferene S. Suitable controls showed that under these conditions, trapping of the released Fe^{2+} in the colored complex with ferene S was sufficiently fast so that it did not affect the measured rates of metal dissociation. The time-dependent decrease in enzyme-bound Fe^{2+} was best described by a single exponential. Non-linear fits of the data yielded pseudo first-order

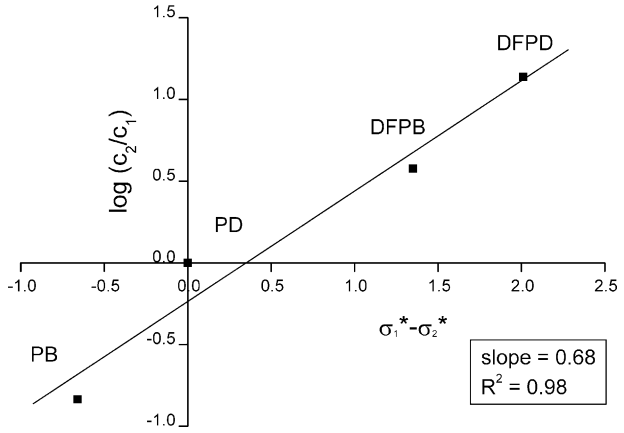

Fig. 7. Analysis of the substituent effect on the C—C bond cleavage selectivity of Glu-69 → Gln mutant. Enzymic substrate conversion and subsequent product quantification via HPLC were performed as described previously [15]. A correlation of the logarithmic product ratio of methylglyoxal (c_2) and acetate (c_1) and the corresponding substituent $\Delta\sigma^*$ values ($= \sigma_1^* - \sigma_2^*$) is given. The substituent Taft factors σ^* are from the literature [15]. In the case of benzoylic substrates, the relevant ratio is phenylglyoxal (c_2) and benzoate (c_1). Note that c_2 and c_1 result from C—C bond cleavage at different positions which can be distinguished in asymmetric β-diketone substrates. Results obtained with 1-phenyl-1,3-butanedione (PB), 4,4-difluoro-1-phenyl-1,3-butanedione (DFPB), 2,4-pentanedione (PD), and 1,1-difluoro-2,4-pentanedione (DFPD) are indicated in the Figure.

rate constants of Fe^{2+} release (k_{rel}). The value of k_{rel} for Glu-69 → Gln ($0.2 \pm 0.03\,min^{-1}$) was twice that of the wild-type ($0.1 \pm 0.03\,min^{-1}$), suggesting that the metal cofactor is bound 'less tightly' in the mutant. Faster dissociation of Fe^{2+} from the metal site of the mutant provides a convincing explanation for the relative Fe^{2+} content in purified enzyme preparations which was always lower in Glu-69 → Gln (40–60%) than wild-type (80–100%).

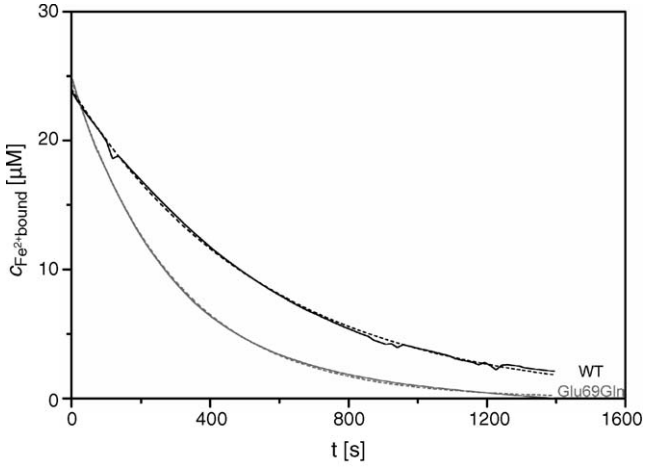

Fig. 8. Kinetics of Fe^{2+} dissociation from the active sites of wild-type Dke1 and Glu-69 → Gln mutant. Experiments were performed at 25 °C in 20 mM Tris/HCl buffer, pH 7.5, using an initial concentration of Fe^{2+} containing active sites ($c_{Fe^{2+}}$ bound) of 25 μM. The time-dependent release of Fe^{2+} was measured with the colorimetric assay. Dashed lines show a single exponential fit to the data.

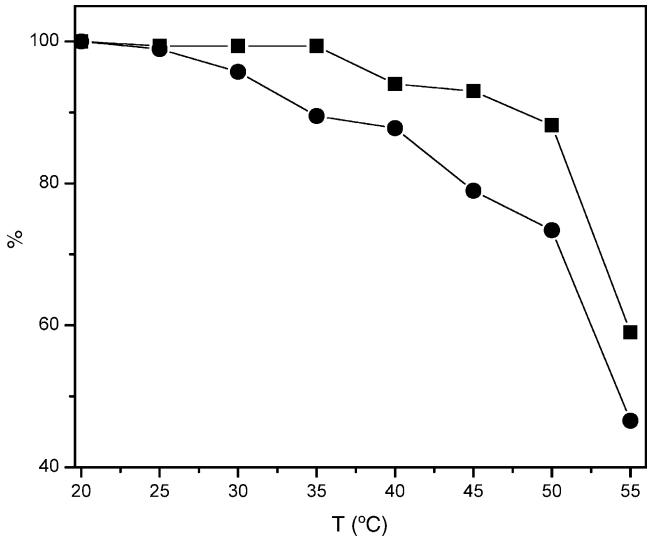

Fig. 9. Thermal denaturation of apo-forms of wild-type Dke1 (squares) and Glu-69 → Gln mutant (circles) recorded by CD spectroscopy. Experiments were carried out at a constant protein concentration of 0.25 mg mL^{-1}. The residue molar ellipticity at 230 nm was used to monitor the loss of β-sheet secondary structure, and results are expressed as percentage of the value measured at 20 °C.

3.6. Thermal denaturation

Changes in molar ellipticity at 230 nm, expressed as percentage of the start value at 20 °C, were used to monitor modifications at the level of the β-sheet secondary structure content in apo-forms of wild-type Dke1 and the Glu-69 → Gln mutant brought about by thermal denaturation in the range 20–95 °C. The results are summarized in Fig. 9.

The observed temperature profiles show that thermally induced denaturation of wild-type and Glu-69 → Gln mutant is clearly not a simple all-in-one process. Significant decreases in the value of Θ took place already at low temperatures (wild-type: ≤40 °C; mutant: ≤30 °C) whereas strong melting of secondary structure was found at considerably higher temperatures (wild-type: ≥50 °C; mutant: ≥40 °C). Dke1 is a functional homotetramer, and a multi-step pathway of thermal denaturation is probably to be expected for a protein with a native quaternary structure. In the absence of further information regarding the occurrence of distinct unfolding intermediates, interpretation of the temperature profiles in Fig. 9 is not warranted. However, their comparative analysis reveals that the mutant was significantly less stable than the wild-type, reflected by the fact that both the onset of denaturation and the maximum melting of β-sheet secondary structure took place at considerably lower temperatures for Glu-69 → Gln ($\Delta T \approx 10$ °C).

4. Conclusions

Mutation of Glu-69 into glutamine is a largely conservative side chain substitution in regard to the catalytic function of Dke1. Only minimal perturbations in the reaction coordinate for the wild-type, as defined in Scheme 1, are caused by the site-directed replacement. Considering the strong conservation pattern for Glu-69 positional homologues in related cupin met-

alloenzymes and in the light of the obviously crucial catalytic role of the respective residue in quercetin dioxygenase [14], this finding is unexpected and very interesting. Obviously Glu-69 is not part of a conserved *catalytic* oxygenase signature. Furthermore its effect on metal-binding, which is mirrored by a two-fold faster Fe^{2+} loss, is only moderate and does not suggest a direct involvement in binding. By comparison, substitution of metal-binding histidines in Dke1 lead to destruction of the metal binding site (S. Leitgeb, G.D.S. and B.N., unpublished data, 2005). Comparison of the results of this paper and reports in the literature [14] suggests that roles for Glu-69 are probably multiple and not always essential, as in Dke1.

Acknowledgements

The technical assistance of Daniela Rainer is gratefully acknowledged. B.N. and S.D. acknowledge Project 14/2004 in the frame of the scientific collaboration between Austria and Italy Ministries.

References

[1] M. Costas, M.P. Mehn, M.P. Jensen, L. Que Jr., Chem. Rev. 104 (2004) 939–986.
[2] E.L. Hegg, L. Que Jr., Eur. J. Biochem. 250 (1997) 625–629.
[3] J.M. Dunwell, A. Purvis, S. Khuri, Phytochemistry 65 (2004) 7–17.
[4] J.M. Dunwell, A. Culham, C.E. Carter, C.R. Sosa-Aguirre, P.W. Goodenough, Trends Biochem. Sci. 26 (2001) 740–746.
[5] P.J. Gane, J.M. Dunwell, J. Warwicker, J. Mol. Evol. 46 (1998) 488–493.
[6] E. Woo, J. Dunwell, P.W. Goodenough, A.C. Marvier, R.W. Pickersgill, Nat. Struct. Biol. 7 (2000) 1036–1040.
[7] A. Tanner, S. Bornemann, J. Bacteriol. 182 (2002) 5271–5273.
[8] W. Fu, P. Oriel, Extremophiles 2 (1998) 439–446.
[9] Y.H. Kwon, M.H. Stipanuk, Am. J. Physiol. Endocrinol. Metab. 280 (2001) E804–E815.
[10] T.C. Pochapsky, S.S. Pochapsky, T. Ju, H. Mo, F. Al-Mjeni, M.J. Maroney, Nat. Struct. Biol. 9 (2002) 966–972.
[11] F. Fusetti, K.H. Schröter, R.A. Steiner, P.I. van Noort, T. Pijning, H.J. Rozeboom, K.H. Kalk, M.R. Egmond, B.W. Dijkstra, Structure 10 (2002) 259–268.
[12] G. Straganz, L. Brecker, H.J. Weber, W. Steiner, D.W. Ribbons, Biochem. Biophys. Res. Commun. 297 (2002) 232–236.
[13] G.D. Straganz, A. Glieder, L. Brecker, D.W. Ribbons, W. Steiner, Biochem. J. 369 (2003) 573–581.
[14] R.A. Steiner, K.H. Kalk, B.W. Dijkstra, Proc. Natl. Acad. Sci. U.S.A. 99 (2002) 16625–16630.
[15] G. Straganz, H. Hofer, W. Steiner, B. Nidetzky, J. Am. Chem. Soc. 126 (2004) 12202–12203.
[16] G. Straganz, B. Nidetzky, J. Am. Chem. Soc. 127 (2005) 12306–12314.
[17] G.R. Stranzl, X-ray crystal structure of acetylacetone-cleaving dioxygenase of *A. johnsonii* and NMR evidence for a strong short hydrogen bond in the active site of HbHNL. Ph.D. thesis, Karl Franzens University of Graz, Graz, Austria, 2002.
[18] W. Wang, B.A. Malcolm, Biotechniques 26 (1999) 680–682.
[19] G. Straganz, A. Slavica, H. Hofer, U. Mandl, W. Steiner, B. Nidetzky, Biocatal. Biotransform. 23 (2005) 261–269.
[20] A. Skerra, T.G. Schmidt, Methods Enzymol. 326 (2000) 271–304.
[21] T. Higgins, Clin. Chem. 27 (1981) 1619–1620.
[22] K. Johnson-Winters, V.M. Purpero, M. Kavana, T. Nelson, G.R. Moran, Biochemistry 42 (2003) 2072–2080.